

# Pre-deposition of iron-based adsorbents on the removal of humic acid using ultrafiltration and membrane fouling

Hailong Tian<sup>1</sup>, Lihua Sun<sup>\*2</sup>, Xi Duan<sup>1</sup>, Xueru Chen<sup>3</sup>, Tianmin Yu<sup>4</sup> and Cuimin Feng<sup>2</sup>

<sup>1</sup>School of Environment and Energy Engineering, Beijing University of Civil Engineering and Architecture, No.1 zhanlanguan Road, Beijing, China

<sup>2</sup>Key Laboratory of Urban Stormwater System & Water Environment, Beijing University of Civil Engineering and Architecture, No.1 zhanlanguan Road, Beijing, China

<sup>3</sup>Beijing General Municipal Engineering Design & Research Institute Co., Ltd, Building 3, No.32, Xizhimen North Street, Haidian District, Beijing, China

<sup>4</sup>Beijing Harbour Real Estate Development Co., Ltd, No.101, Jing Shun Road, Chaoyang District, Beijing, China

(Received August 21, 2016, Revised December 12, 2017, Accepted August 20, 2018)

**Abstract.** The effect of three iron-based adsorbents pre-depositing on ultrafiltration membrane for humic acid (HA) removal and membrane fouling was investigated. The result showed that pre-depositing adsorbents on membrane could not only reduce membrane fouling but also enhance HA removal. The flux was related to the adsorbent dosage and the optimal dosage for pre-deposition was 35.0 g/m<sup>2</sup>. The dissolved organic carbon (DOC) removal of HA was 38.3%, 67.3% and 41.1% respectively when pre-deposited 35.0 g/m<sup>2</sup> FeO<sub>x</sub>H<sub>y</sub>, MnFe<sub>2</sub>O<sub>4</sub> and Fe<sub>3</sub>O<sub>4</sub> on membrane. Different adsorption effect of adsorbents on HA contributed to increasing of the flux at different level. Zeta potential of three adsorbents all decreased after adsorbed HA. The adsorption capacity of the three adsorbents was FeO<sub>x</sub>H<sub>y</sub> > MnFe<sub>2</sub>O<sub>4</sub> > Fe<sub>3</sub>O<sub>4</sub>. Atomic Force Microscopy (AFM) measurement showed the thickness of pre-deposition layers formed by different adsorbents was different. The scanning electron microscope (SEM) detection showed the morphology and compactness of pre-deposition layers formed by different adsorbents was different.

**Keywords:** adsorption; humic acid; filtration flux; membrane fouling; pre-deposition; ultrafiltration

## 1. Introduction

Natural organic matter (NOM), the most important reactive fraction in water, is widely found in ground waters, surface waters, soils and sediments (Woods *et al.* 2011, Qin *et al.* 2012). A major constituent of NOM is humic substances, these being composed of humic acids (HA), fulvic acids and humin. In water, HA is present in the form of dissolved organic matter (Saito *et al.* 2004), and it readily reacts with chlorine in water treatment processes, a reaction that has been found to have a tendency to form disinfection by-products (DBPs) (Aoustin *et al.* 2001, Kabsch-Korbutowicz 2005, Zularisam *et al.* 2006, Xia *et al.* 2004, Mozia and Tomaszewska 2004). Epidemiological studies have shown that there is a potential correlation between the consumption of chlorine disinfection in drinking water and the incidence of bladder cancer, rectal cancer and colon cancer (Nieuwenhuijsen 2005). In addition, DBPs in drinking water may also cause reproductive and developmental side effects (Hwang 2003).

Currently, HA removal methods mainly include activated carbon adsorption, photochemical catalysis and oxidation, strengthened coagulation, ozone oxidation and membrane technology. The use of membrane filtration

processes in potable water production has increased rapidly over the last 10 years, mainly due to its advantages over conventional treatments, such as having a smaller footprint, a compact module and the capacity to handle wide fluctuations in feed quality. To increase our knowledge about fouling in ultrafiltration (UF) of NOM, extensive investigations have been undertaken which have included allochthonous humic substances and autochthonous biopolymers (mainly consisting of protein and polysaccharides), generally believed to be the causes of membrane fouling (Amy 2008, Sutzkover-Gutman *et al.* 2010, Xiao *et al.* 2013, Ma *et al.* 2014). Pre-treatment of feed water by coagulation, adsorption, ion exchange, or chemical oxidation has been previously investigated as a strategy for reducing membrane fouling by NOM (Carroll *et al.* 2000, Mozia *et al.* 2004, 2005, Mavrov *et al.* 1998, Ha *et al.* 2004, Hyung *et al.* 2000, Haberkamp *et al.* 2007, Humbert *et al.* 2007). These processes, however, increase the processing unit as well as the processing cost. Recent investigations have proposed that the pre-deposition of adsorbents on the surface of ultrafiltration membranes can form a protective layer which will reduce membrane fouling due to ensuring the removal efficiency of the pollutants (Ye *et al.* 2006). The action of adding a loose pre-coating layer on the membrane will not result in serious membrane fouling, however the pre-coating layer will not only adsorb pollutants, it will also effectively filter or intercept pollutants (Lin *et al.* 2012). Compared with traditional UF

\*Corresponding author, Ph.D.  
E-mail: sunlihuashd@163.com

methods, the addition of a pre-coating layer can improve the removal effect of particles having different molecular weights, surface charge and hydrophobicity of the organic matter, especially on small organic molecules. A large number of materials have exhibited excellent pre-coating effects, such as chitosan (Yoon *et al.* 2006) and nano titanium dioxide (Huang *et al.* 2008).

In this study, to investigate the effects pre-deposition of adsorbents have on an ultrafiltration membrane, their removal of HA and their effect on membrane fouling behavior, three iron based materials ( $\text{FeO}_x\text{H}_y$ ,  $\text{MnFe}_2\text{O}_4$  and  $\text{Fe}_3\text{O}_4$ ) were selected and pre-deposited on to an ultrafiltration membrane. As per the standards of reclaimed water quality (SL 368-2006, China), 20 mg/L HA was used to simulate reclaimed water having low organic pollution. Results from this study will clarify the mechanisms of interaction between the pre-deposition materials, contaminants and the ultrafiltration membrane. To undertake this study, an advanced purification method of pre-deposition adsorption-ultrafiltration for wastewater treatment was constructed which provided basic support for the safe reuse of reclaimed water.

## 2. Methods

### 2.1 Chemical agents and materials

All chemicals used in this study were analytical grade. Deionized (DI) water was used to prepare all solutions, and the pH of the solutions was adjusted using 0.10 mol/L HCl and 0.10 mol/L NaOH. 1.0 g/L humic acid (HA, Aldrich, USA) was prepared and stored at 4°C for analysis. The three materials used in this study were  $\text{MnFe}_2\text{O}_4$ ,  $\text{Fe}_3\text{O}_4$  (both supplied by Beijing Dk Nano technology Co., Ltd, China; basic characteristics are shown in Table 1) and  $\text{FeO}_x\text{H}_y$ , prepared by reacting iron chloride hexahydrate ( $\text{FeCl}_3 \cdot 6\text{H}_2\text{O}$ ) and NaOH at the equivalent  $\text{Fe}^{3+}/\text{OH}^-$  molar ratio of 1:3 (He *et al.* 2015). A polyvinylidene fluoride (PVDF) flat sheet UF membrane (supplied by Ande Membrane Separation Technology & Engineering, Beijing, Co., Ltd, China) was used as the membrane in this study, the characteristics of this sheet are shown in Table 2.

Table 1 Basic characteristics of  $\text{MnFe}_2\text{O}_4$  and  $\text{Fe}_3\text{O}_4$

Adsorbents	Color	Content/%	Particle morphology	Density ( $\text{g}/\text{cm}^3$ )
$\text{Fe}_3\text{O}_4$	black	99.9	spherical	4.8~5.1
$\text{MnFe}_2\text{O}_4$	black	99.9	spherical	5.6~7.3

Table 2 Characteristics of the PVDF membrane

Index	Parameter values
Temperature/ °C	5-38
pH	2-13
Molecular weight cutoff/Da	100000
Effective filtration area/ $\text{cm}^2$	0.45
Working pressure /MPa	0.35

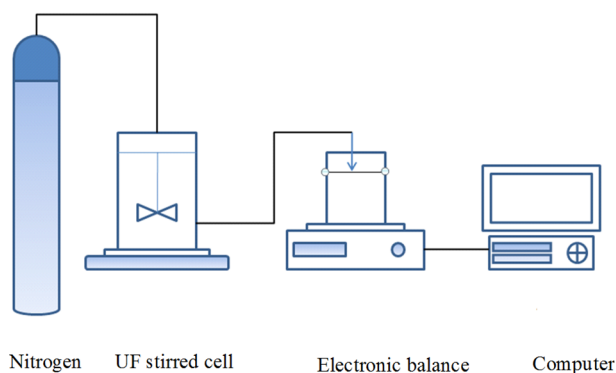


Fig. 1 A schematic diagram of the ultrafiltration test device

### 2.2 UF experiment

In order to remove impurities and production residues, each membrane was immersed in DI water for at least 24 h before being used in the filtration process (Fig. 1). Filtration pressure was applied to the process using nitrogen gas, maintained at 0.10 Mpa throughout the experiment. The simulated water was added to the apparatus and filtered through the membrane fixed at the bottom of a UF stirred cell (8400, Millipore Co., USA). The filtered water passed into a beaker which was continuously weighed using an electronic balance (8400, Millipore Co., USA) and the weight data automatically recorded every minute by computer.

350 mL DI water was initially filtered and its stable permeate flux was recorded as  $J_0$ . Different volumes of  $\text{FeO}_x\text{H}_y$  were then added into a 400 mL beaker containing 350 mL DI water to make different concentrations of solution for the experiment.  $\text{FeO}_x\text{H}_y$  was dispersed using an ultrasonic probe for 5 min before the pH was adjusted to  $7.0 \pm 0.2$ . Once the pH had been adjusted, the working solution was decanted into the UF cell, without a cover, and stirred for 1 min (100 r/min) before being left to settle. After 10 min a pre-deposition layer had formed in the cell, after which 7.0 mL of 1.0 g/L HA was then added to the solution. This solution was left for 30 min, after which the HA solution had been completely dispersed in the  $\text{FeO}_x\text{H}_y$  solution. Finally, the solution was filtered and the flux was recorded as  $J$ . Normalized flux  $J/J_0$  as a function of time was calculated to show flux decline results from this experiment. The filtration experiment was repeated 3 times and the mean flux value was recorded. The experiment of pre-deposition different concentrations of  $\text{MnFe}_2\text{O}_4$  and  $\text{Fe}_3\text{O}_4$  was as the same as  $\text{FeO}_x\text{H}_y$ .

### 2.3 Analytical methods

Molecular weight distribution was determined by Gel Permeation Chromatography (GPC, Agilent Technologies, USA; Detector: UV<sub>254</sub>; Column: TSK; Temperature: 25°C) (Ma *et al.* 2014). Micro-structure of the adsorbents was measured by Specific surface analyzer (BELSORP-miniII, NIKKISO GROUP, Japan). Zeta potential and particle size were measured by Zeta sizer (Nano ZS, Malvin, England).

DOC was measured using a total organic carbon analyzer (TOC-VCPH, SHIMADZU Co., Japan). The pre-deposited membranes were scanned using a scanning electron microscope (S-3000N, Hitachi High-Technologies Co., Japan) and a high resolution atomic force microscope (Multimode-8, BrukerCo., USA).

### 3. Results and discussion

#### 3.1 Adsorbent concentration and HA Flux

To investigate the effect adsorbent concentration has on HA flux, pre-deposited concentrations of  $\text{MnFe}_2\text{O}_4$ ,  $\text{Fe}_3\text{O}_4$  and  $\text{FeO}_x\text{H}_y$  were applied to the membrane and the flux was monitored over a 10 minute period. Results from this analysis (Fig. 2) show that flux initially increased before decreasing as the concentration of the adsorbents increased. The optimal concentration for the three adsorbents was 105.0, 35.0 and 35.0  $\text{g/m}^2$  for  $\text{MnFe}_2\text{O}_4$ ,  $\text{Fe}_3\text{O}_4$  and  $\text{FeO}_x\text{H}_y$ , respectively. Compared with the blank samples, the flux increased by 48.0%, 38.7% and 49.8% after 10 min, respectively. Results for  $\text{MnFe}_2\text{O}_4$  recorded a higher flux when the  $\text{MnFe}_2\text{O}_4$  concentration was 105.0  $\text{g/m}^2$ . But the difference of  $J/J_0$  with 35.0 and 105.0  $\text{g/m}^2$  was not big. And the optimal dosage of 35.0  $\text{g/m}^2$  was recorded for the other two adsorbents. Therefore 35.0  $\text{g/m}^2$  was chosen as the optimal adsorbent concentration for subsequent analysis comparing the suitability of the different adsorbents.

#### 3.2 Removal of HA

The removal of dissolved organic carbon (DOC) of HA from the water samples using an untreated filter and filters with 35.0  $\text{g/m}^3$  for the three adsorbents is shown in Table 3. The results show that the untreated UF accounted for 33.1% of removal. After treating the membranes with the optimal concentration of adsorbents, DOC removal was 38.4%, 66.9% and 41.0% for  $\text{MnFe}_2\text{O}_4$ ,  $\text{Fe}_3\text{O}_4$  and  $\text{FeO}_x\text{H}_y$ , respectively. The removal effect of pre-depositing adsorbents on DOC was  $\text{MnFe}_2\text{O}_4 > \text{Fe}_3\text{O}_4 > \text{FeO}_x\text{H}_y$ .

The molecular weight (MW) distribution of HA before and after treatment was also investigated by Gel Permeation Chromatography (GPC). Results in Figure 3 show that the MW distribution of the raw water sample ranged from 2181-26222 Da, and that the MW distribution of HA using an untreated filter membrane was 2367-24956 Da; the peak response for the untreated membrane was lower, indicating that the UF intercepted the majority of HA molecules, especially the medium sized molecules. Results for the MW distribution of HA after pre-deposition on the membrane ( $\text{FeO}_x\text{H}_y$ +UF,  $\text{MnFe}_2\text{O}_4$ +UF and  $\text{Fe}_3\text{O}_4$ +UF) were 2287-22347 Da, 2244-20124 Da and 2244-19989 Da, respectively. The peak MW distribution of the raw water sample was about 10671 Da (Fig. 3); this peak declined for the UF treatment, and subsequently for each adsorbent on the UF. The optimum result (9432 Da) was recorded for  $\text{Fe}_3\text{O}_4$  +UF. HA removal, calculated using the peak area, was 14.5%, 29.4%, 54.1% and 38.9% for UF,  $\text{FeO}_x\text{H}_y$ +UF,  $\text{MnFe}_2\text{O}_4$  +UF and  $\text{Fe}_3\text{O}_4$ +UF, respectively. This result further demonstrates that the pre-deposition process was an effective method to alleviate membrane fouling.

Table 3 Adsorbent removal of DOC

	Raw water	UF	$\text{FeO}_x\text{H}_y$ + UF	$\text{MnFe}_2\text{O}_4$ + UF	$\text{Fe}_3\text{O}_4$ + UF
DOC/(mg/L)	10.92	7.31	6.73	3.62	6.44
DOC removal / %	-	33.1	38.4	66.9	41.0

Footnote: The adsorbent concentrations were all 35.0  $\text{g/m}^2$ ; HA = 20 mg/L; pH = 7.0

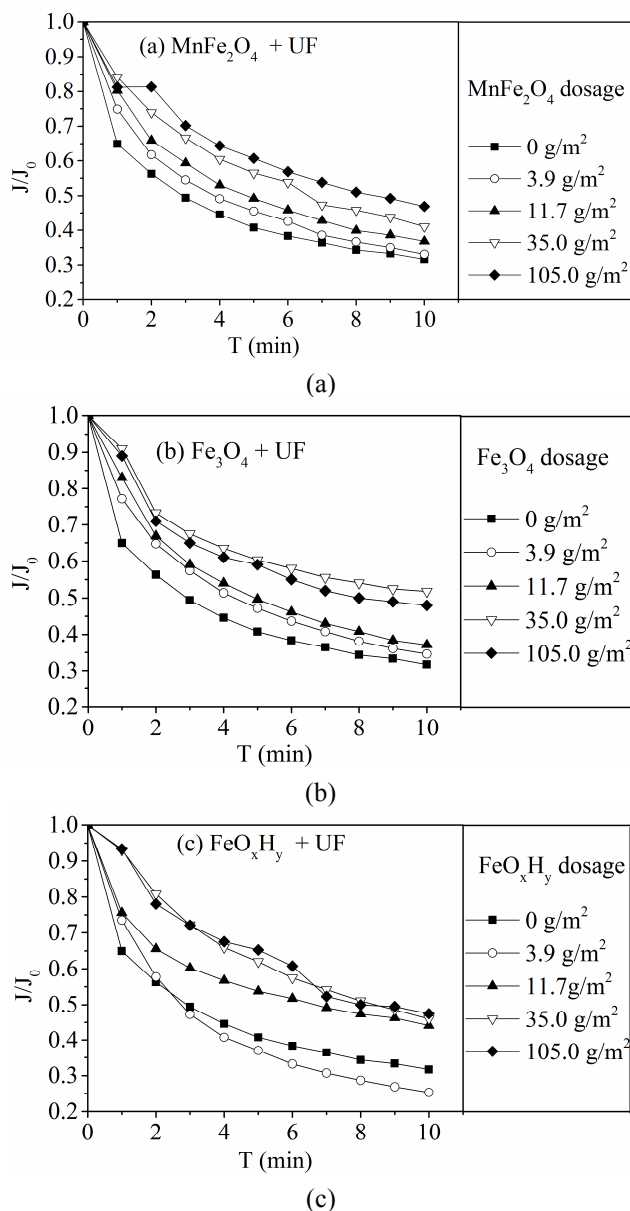


Fig. 2 Normalized flux decline of HA with/without pre-deposition under different concentrations of (a)  $\text{MnFe}_2\text{O}_4$ , (b)  $\text{Fe}_3\text{O}_4$  and (c)  $\text{FeO}_x\text{H}_y$

#### 3.3 Zeta potential

Zeta potential, a frequently used method to obtain surface potential information and to investigate the adsorption of humic substances on the surface charge of metal oxides (Kumpulainen *et al.* 2008, Sharp *et al.* 2006), was recorded before and after adsorption in this study (Table 4). Our results show that the zeta potential of

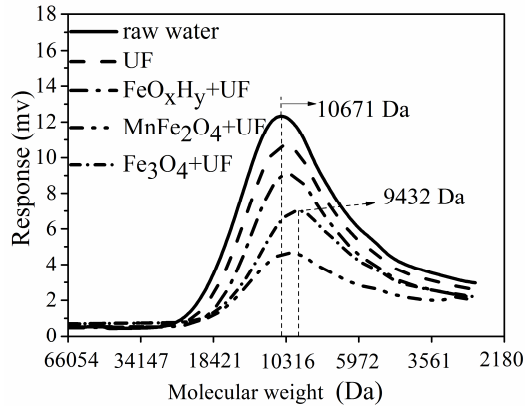


Fig. 3 Molecular weight distribution of HA before and after treatment (The concentration of all adsorbents was 35.0 g/m<sup>2</sup>; HA = 20 mg/L; pH = 7.0)

Table 4 Zeta potential of adsorbents before and after adsorption at pH = 7.0

Adsorbent	FeO <sub>x</sub> H <sub>y</sub>	MnFe <sub>2</sub> O <sub>4</sub>	Fe <sub>3</sub> O <sub>4</sub>
Zeta potential before adsorption (mv)	0.07	-5.45	-1.62
Zeta potential after adsorption (mv)	-8.48	-10.56	-8.72

adsorbents after adsorbing HA were much lower than those before adsorption. The change of Zeta potential was FeO<sub>x</sub>H<sub>y</sub> > Fe<sub>3</sub>O<sub>4</sub> > MnFe<sub>2</sub>O<sub>4</sub>. The change of Zeta of the three adsorbents before and after adsorption indicated that they all adsorbed more HA molecules containing a negative charge.

The adsorption of adsorbents on HA can be mainly characterized by electrostatic interactions and ligand exchange. As previously reported (And *et al.* 2005), most iron oxide particles were hydrated, and M-OH groups covered their surfaces. The M-OH sites on the particle surfaces reacted with H<sup>+</sup> or OH<sup>-</sup> in the solution, thus generating positive M-OH<sub>2</sub><sup>+</sup> (M-OH + H<sup>+</sup> ⇌ M-OH<sub>2</sub><sup>+</sup>) or negative M-O<sup>-</sup> (M-OH + OH<sup>-</sup> ⇌ M-O<sup>-</sup> + H<sub>2</sub>O) on the surface of the adsorbents via protolytic reactions (Cornell *et al.* 2003, Illés *et al.* 2006, Hajdú *et al.* 2012, Buffle and van Leeuwen 1992). Carboxyl groups contained in HA therefore reacted with M-OH<sub>2</sub><sup>+</sup> and M-O<sup>-</sup>, having the following formulae:

### 3.4 Micro-structure of the adsorbents

In order to explore the mechanisms of pre-deposition on the ultrafiltration membrane process, particle size and micro structure of the three adsorbents were determined (Table 5). Results for Brunner–Emmet–Teller (BET) show a noticeable difference between the adsorbents, with FeO<sub>x</sub>H<sub>y</sub> (180.52 m<sup>2</sup>/g) recording the greatest and Fe<sub>3</sub>O<sub>4</sub> (10.71 m<sup>2</sup>/g) having the lowest. Specific surface area was proportional to the adsorption ability, and the BET surface area of FeO<sub>x</sub>H<sub>y</sub> was 2.48 times bigger than MnFe<sub>2</sub>O<sub>4</sub> and 16.9 times bigger than Fe<sub>3</sub>O<sub>4</sub>, showing that the adsorption capacity of the three adsorbents was FeO<sub>x</sub>H<sub>y</sub> > MnFe<sub>2</sub>O<sub>4</sub> > Fe<sub>3</sub>O<sub>4</sub>. The order of the mean pore size of the adsorbents was MnFe<sub>2</sub>O<sub>4</sub> > Fe<sub>3</sub>O<sub>4</sub> > FeO<sub>x</sub>H<sub>y</sub>.

Table 5 Micro-structure of the adsorbents

Adsorbent	Mean particle size (nm)	BET surface area (m <sup>2</sup> /g)	Total pore volume (mL/g)	Mean pore size (nm)
FeO <sub>x</sub> H <sub>y</sub>	1200.92	180.52	0.10	2.30
MnFe <sub>2</sub> O <sub>4</sub>	300.92	72.85	0.01	12.30
Fe <sub>3</sub> O <sub>4</sub>	201.32	10.71	0.02	8.37

Table 6 Membrane roughness for the different samples

Sample	R <sub>a</sub> /nm	R <sub>q</sub> /nm	Z/nm
UF	116.52	146.91	902.04
HA + UF	71.53	88.42	554.34
FeO <sub>x</sub> H <sub>y</sub> + UF	223.43	335.22	3873.25
HA + FeO <sub>x</sub> H <sub>y</sub> + UF	211.92	324.35	3772.46
MnFe <sub>2</sub> O <sub>4</sub> + UF	153.44	207.27	2042.41
HA + MnFe <sub>2</sub> O <sub>4</sub> + UF	139.06	190.11	1973.20
Fe <sub>3</sub> O <sub>4</sub> + UF	153.27	202.32	2237.19
HA + Fe <sub>3</sub> O <sub>4</sub> + UF	147.03	186.63	2130.04

Footnote: (The concentration of all adsorbents was 35.0 g/m<sup>2</sup>; HA = 20 mg/L; pH = 7.0).

R<sub>a</sub>: Average roughness, the arithmetic mean value of the absolute value of the height of each point of the membranes relative to the zero plane. R<sub>q</sub>: Root mean square roughness, the root mean square of the height of each point of membranes relative to the zero plane. Z: the maximum height of the profile, which is between the diaphragm surface peak and valley line distance.

Flux results in Figure 2 showed HA treated by FeO<sub>x</sub>H<sub>y</sub> + UF to not be the most efficient, however FeO<sub>x</sub>H<sub>y</sub> had the best adsorption ability. This result can be explained by FeO<sub>x</sub>H<sub>y</sub> recording the greatest mean particle size and smallest mean pore size. Although a large particle size is not conducive to the retention of HA molecules, the large size of FeO<sub>x</sub>H<sub>y</sub> made the gap between the particles large, therefore enabling HA molecules to easily pass through the gaps. In addition, the small pore size was not conducive to the adsorption of large HA molecules, thus adsorption of HA by FeO<sub>x</sub>H<sub>y</sub> was worse than that of Fe<sub>3</sub>O<sub>4</sub>. As MnFe<sub>2</sub>O<sub>4</sub> and Fe<sub>3</sub>O<sub>4</sub> particle sizes were smaller, the space between particles was therefore smaller which increased the contact opportunity between HA molecules and the adsorbent particles. At the same time, their mean pore sizes were greater than those of FeO<sub>x</sub>H<sub>y</sub>, which is beneficial for the adsorption of large HA molecules. Results from this analysis therefore show that adsorbents with a large specific surface area and small particle size were beneficial to the pre-deposition process.

### 3.5 Membrane roughness

Atomic Force Microscopy (AFM) measurement was undertaken on two areas of each membrane with adsorbents pre-deposited. Results from this analysis (Fig. 4 and Table 6) show that FeO<sub>x</sub>H<sub>y</sub>+UF recorded the greatest roughness (R<sub>a</sub>=223.43, R<sub>q</sub>=335.22, Z=3873.25), followed by MnFe<sub>2</sub>O<sub>4</sub>

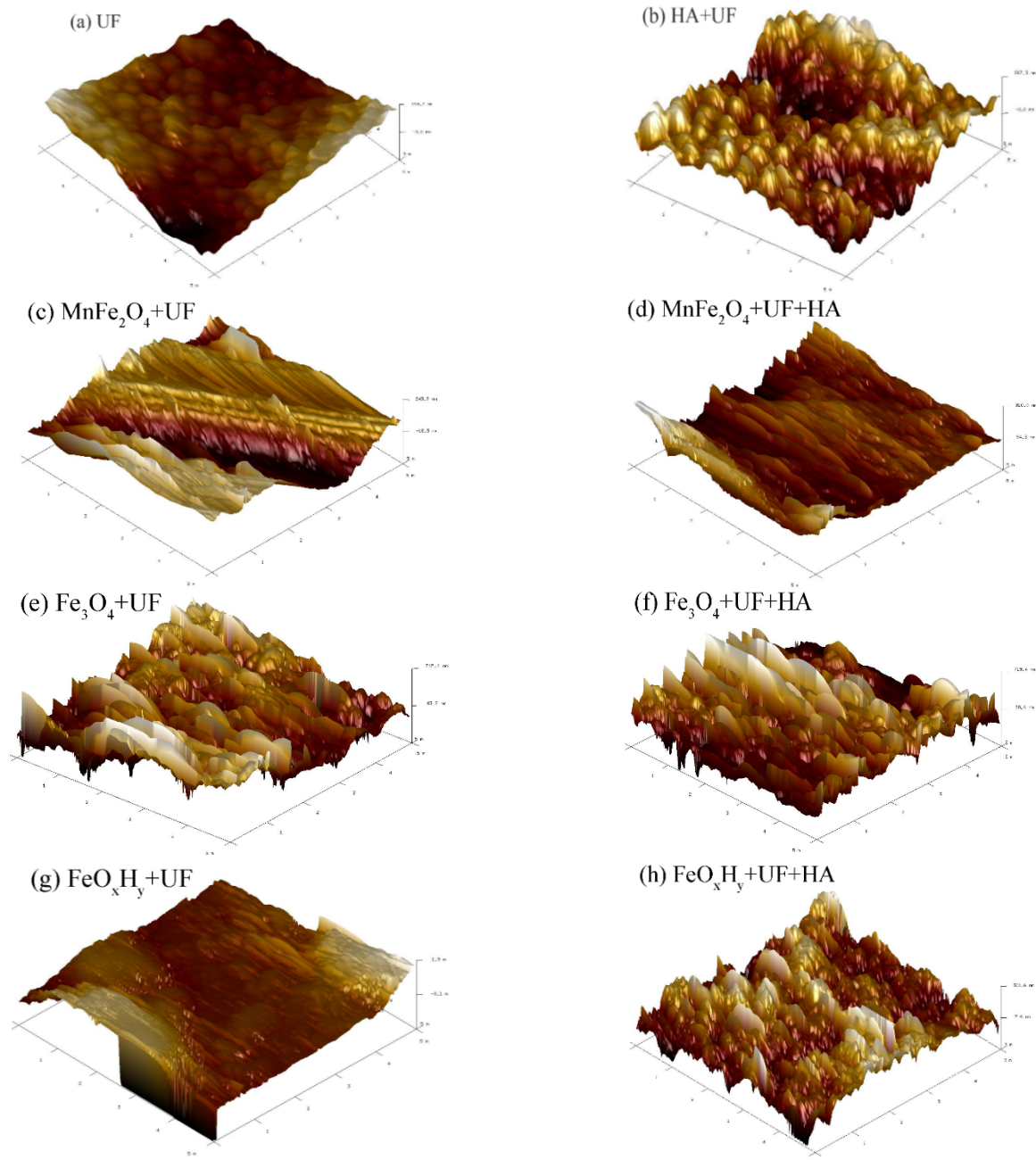


Fig. 4 3-D shape of membranes with or without pre-deposition: (a) UF, (b) HA+UF, (c)  $\text{MnFe}_2\text{O}_4$ +UF, (d)  $\text{MnFe}_2\text{O}_4$ +UF+HA, (e)  $\text{Fe}_3\text{O}_4$ +UF, (f)  $\text{Fe}_3\text{O}_4$  + UF+HA, (g)  $\text{FeO}_x\text{H}_y$ +UF and (h)  $\text{FeO}_x\text{H}_y$ +UF+HA (The concentration of all adsorbents was  $35.0 \text{ g/m}^2$ ; HA =  $20 \text{ mg/L}$ ; pH = 7.0)

+UF,  $\text{Fe}_3\text{O}_4$ +UF, UF and HA+UF. Interestingly, the roughness of UF + HA was higher than that of UF. After treatment with HA, the roughness ( $R_a$ ,  $R_q$ , Z) of HA+ $\text{FeO}_x\text{H}_y$  + UF, HA+ $\text{MnFe}_2\text{O}_4$  + UF and HA+ $\text{Fe}_3\text{O}_4$  + UF were lower than those of  $\text{FeO}_x\text{H}_y$ +UF,  $\text{MnFe}_2\text{O}_4$ +UF and  $\text{Fe}_3\text{O}_4$ +UF, respectively. This result may be due to the interception and adsorption of deposition on HA molecules which resulted in the sedimentary structure to become denser.  $R_a$ ,  $R_q$  and Z of  $\text{MnFe}_2\text{O}_4$  and  $\text{Fe}_3\text{O}_4$  pre-depositions were much smaller than that of  $\text{FeO}_x\text{H}_y$ , indicating that they were smoother and thinner.

In addition,  $\text{MnFe}_2\text{O}_4$  and  $\text{Fe}_3\text{O}_4$  particles were smaller than those of  $\text{FeO}_x\text{H}_y$ , resulting in their pre-deposition

layers being thinner and denser. HA therefore had a greater possibility of colliding with  $\text{MnFe}_2\text{O}_4$  and  $\text{Fe}_3\text{O}_4$  particles, thus increasing their potential to be adsorbed. Our results indicate that it was easiest for  $\text{Fe}_3\text{O}_4$  to adsorb HA molecules, followed by  $\text{MnFe}_2\text{O}_4$  and  $\text{FeO}_x\text{H}_y$ ; HA removal was therefore determined by adsorption capacity and adsorption opportunity together.

### 3.6 SEM pictures for the different membranes

Scanning electron microscopy (SEM) detection was undertaken on different areas of each membrane during deposition, the most representative images are shown in

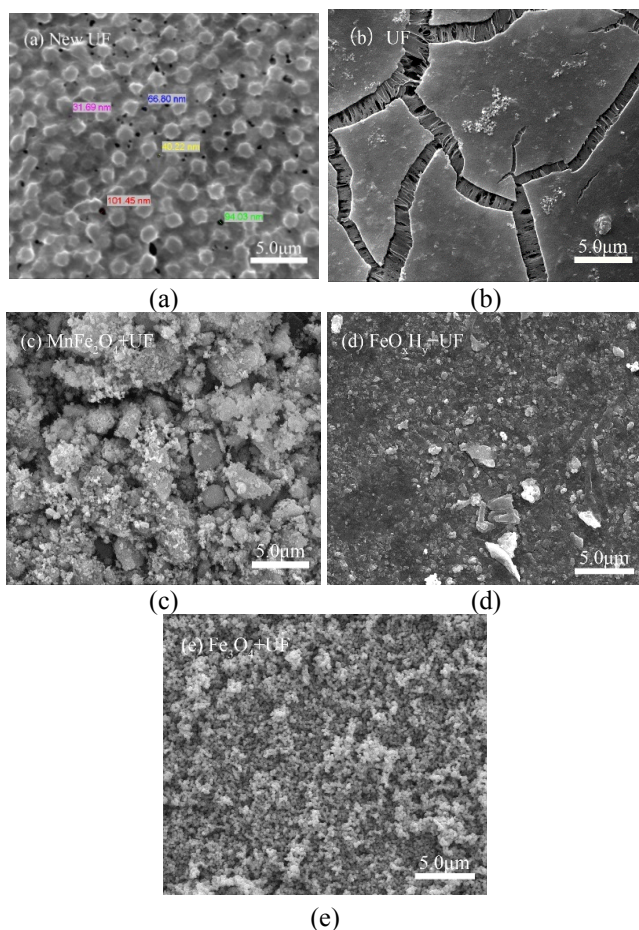


Fig. 5 SEM of membranes with and without pre-deposition: (a) new UF, (b) UF, (c)  $\text{MnFe}_2\text{O}_4$  + UF, (d)  $\text{FeO}_x\text{H}_y$  + UF and (e)  $\text{Fe}_3\text{O}_4$  + UF. (The concentration of all adsorbents was  $35.0 \text{ g/m}^2$ ; HA =  $20 \text{ mg/L}$ ; pH = 7.0).

Figure 5. Results show that the pore size distribution of new UF was mainly 30-100 nm (Fig. 5a), this being small enough to hold the three adsorbents. It can be seen in Figure 5b that HA molecules formed a cake layer of over the membrane which contributed to membrane clogging and a decline in flux results. Pre-deposition of  $\text{MnFe}_2\text{O}_4$  on the membrane resulted in a certain particle structure, with agglomeration of particles occurring (Fig. 5c). Pre-deposition of  $\text{FeO}_x\text{H}_y$  on the membrane resulted in a lack of a granular structure for the particles; with a large number of particles, there were no rules for agglomeration and a rough deposition layer occurred (Fig. 5d). Pre-deposition of  $\text{Fe}_3\text{O}_4$  resulted in a complete crystal structure and alignment of the particles, thus resulting in a dense and smooth deposition layer (Fig. 5e). Small voids between the particles resulted in  $\text{Fe}_3\text{O}_4$  having the biggest opportunity to collide with and adsorb HA, followed by  $\text{MnFe}_2\text{O}_4$  and  $\text{FeO}_x\text{H}_y$ .

### 3.7 Pre-deposition mechanism

The pre-deposition mechanism proposed by Galjaard *et al.* (2001) was taken as the mechanism used in this study (Fig. 6). It is believed that the majority of HA molecules passed through the membrane pores during simple ultrafiltration; any interception of HA molecules on the

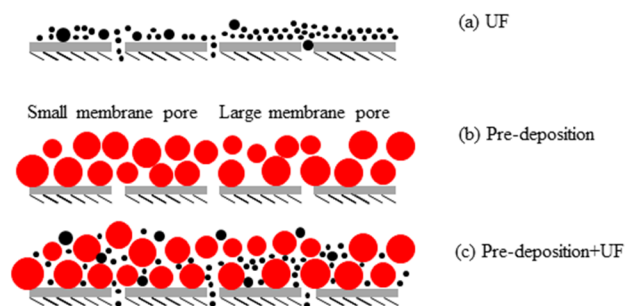


Fig. 6 Schematic diagram of the pre-deposition mechanism

membrane surface was due to membrane holes being blocked by HA with large MWs, thus resulting in HA molecules accumulating around the blocked holes and a subsequent decline in the membrane flux (Fig. 6a). The adsorbent particles deposited on the membrane surface before UF. There were large gaps between particles (Figure 4b). A large number of HA molecules were trapped in the pre-deposition layer during filtration. Large WM HA was easy to be trapped especially. But it would not have a big impact on the penetration of the de-position layer due to the spatial structure of deposition layer which provided a variety of channels for HA molecules. The interception and adsorption of pre-deposition on large MW HA avoided the membrane pore blockage and increased the membrane flux. The rejection and adsorption of pre-deposition on small MW HA contributed to the improvement of water quality (Figure 4c). After several cycles, the membrane was hydraulic backwashed. The adsorbent was collected from backwash water. The adsorbent was treated by thermal regeneration (Peng *et al.* 2006), which will be explored in future.

## 4. Conclusions

The pre-deposition effect of three iron based adsorbent with different concentrations on HA removal and membrane fouling was investigated by many means.

- Our results show that pre-deposition with the adsorbents can protect the filter membrane from being fouled with organic material, and therefore increasing the flux. Flux results for each adsorbent varied, with optimal concentrations of pre-deposition on the UF being  $35.0 \text{ g/m}^2$ .

- GPC detection result showed that flux increase was related to influent water quality. Compared with direct UF, pre-deposition iron based adsorbents on membrane can greatly reduce the concentration of humic acid.

- The adsorption ability and contact chance determined the adsorption effect of the pre-deposition layer on HA. The adsorption capacity of the three adsorbents was  $\text{FeO}_x\text{H}_y > \text{MnFe}_2\text{O}_4 > \text{Fe}_3\text{O}_4$ . The order of contact chance of the adsorbents with HA was  $\text{Fe}_3\text{O}_4 > \text{MnFe}_2\text{O}_4 > \text{FeO}_x\text{H}_y$ . The AFM and SEM analysis further confirmed it.

- Further investigations need to be done, such as the effect of pre-deposition on different HA concentration, the recovery of adsorbents and the influence of different ions on pre-deposition and so on.

## Acknowledgments

This work was supported by the Funds for the National Natural Science Foundation of China (Grant No. 51678027).

## References

- Amy, G. (2008), "Fundamental understanding of organic matter fouling of membranes", *Desalination*, **231**(1), 44-51.
- And, L.C. and Sengupta, A.K. (2005), "Arsenic removal using polymer-supported hydrated iron(III) oxide nanoparticles: role of donnan membrane effect", *Environ. Sci. Technol.* **39**(17), 6508.
- Aoustin, E., Schäfer, A.I., Fane, A.G. and Waite, T.D. (2001), "Ultrafiltration of natural organic matter", *Separat. Purif. Technol.*, **22-23**(1-3), 63-78.
- Buffle, J. and van Leeuwen, H.P. (1992), *Environmental Particles*. Lewis Publishers, Florida, U.S.A.
- Carroll, T., King, S., Gray, S.R., Bolto, B.A. and Booker, N.A. (2000), "The fouling of microfiltration membranes by NOM after coagulation treatment", *Water Res.*, **34**(11), 2861-2868.
- Cornell, R.M. and Schwertman, U. (2003), *The Iron Oxides: Structure, Properties, Reactions, Occurrences and Uses, Second ed*, Wiley, U.S.A.
- Galjaard, G., Buijs, P., Beerendonk, E., Schoonenberg, F. and Schippers, J.C. (2001), "Pre-coating (epce®) of membranes for direct treatment of surface water", *Desalination*, **139**(01), 305-316.
- Ha, T.W., Choo, K.H. and Choi, S.J. (2004), "Effect of chlorine on adsorption/ultrafiltration treatment for removing natural organic matter in drinking water", *J. Colloid and Interface Sci.*, **274**(2), 587-593.
- Haberkamp, J., Ruhl, A.S., Ernst, M. and Jekel, M. (2007), "Impact of coagulation and adsorption on DOC fractions of secondary effluent and resulting fouling behaviour in ultrafiltration", *Water Res.*, **41**(17), 3794-3802.
- Hajdú, A., Szekeres, M., Tóth, I.Y., Bauer, R.A., Mihály, J., Zupkó, I. and Tombácz, E. (2012), "Enhanced stability of polyacrylate-coated magnetite nanoparticles in biorelevant media", *Colloids Surfaces B Biointerfaces*, **94**(6), 242-249.
- He, Z., Liu, R., Liu, H. and Qu, J. (2015), "Adsorption of Sb(III) and Sb(V) on Freshly Prepared Ferric Hydroxide (FeOxHy)", *Environ. Eng. Sci.*, **32**(2), 95.
- Huang, X., Leal, M. and Li, Q. (2008), "Degradation of natural organic matter by TiO<sub>2</sub> photocatalytic oxidation and its effect on fouling of low-pressure membranes", *Water Res.*, **42**(4-5), 1142-1150.
- Humbert, H., Gallard, H., Jacquemet, V. and Croué, J.P. (2007), "Combination of coagulation and ion exchange for the reduction of UF fouling properties of a high DOC content surface water", *Water Res.*, **41**(17), 3803-3811.
- Hwang, B.F. and Jaakkola, J.J. (2003), "Water chlorination and birth defects: A systematic review and meta-analysis", *Arch. Environ. Health*, **58**(2), 83-91.
- Hyung, H., Lee, S., Yoon, J. and Lee, C. (2000), "Effect of preozonation on flux and water quality in ozonation-ultrafiltration hybrid system for water treatment", *Ozone Sci. Eng.*, **22**(6), 637-652.
- Illés, E. and Tombácz, E. (2006), "The effect of humic acid adsorption on pH-dependent surface charging and aggregation of magnetite nanoparticles", *J. Colloid Interface Sci.*, **295**(1), 115-123.
- Kabsch-Korbutowicz, M. (2005), "Effect of Al coagulant type on natural organic matter removal efficiency in coagulation/ultrafiltration process", *Desalination*, **185**(1-3), 327-333.
- Kumpulainen, S., Kammer, F.V.D. and Hofmann, T. (2008), "Humic acid adsorption and surface charge effects on schwertmannite and goethite in acid sulphate waters", *Water Res.*, **42**(8-9), 2051-2060.
- Lin, C.J., Cheng, A.C., Lin, Y.F., Lee, D.J. and Guo, W.M. (2012), "Dense membranes pre-coated with aluminium tridecamer (Al<sub>13</sub>) for water treatment", *Desalination*, **284**(2), 349-352.
- Ma, B., Yu, W., Liu, H. and Qu, J. (2014), "Effect of low dosage of coagulant on the ultrafiltration membrane performance in feedwater treatment", *Water Res.*, **51**(6), 277-283.
- Mavrov, V., Chmiel, H., Kluth, J., Meier, J., Heinrich, F., Ames, P., Backes, K. and Usner, P. (1998), "Comparative study of different MF and UF membranes for drinking water production", *Desalination*, **117**(1-3), 189-196.
- Mozia, S. and Tomaszewska, M. (2004), "Treatment of surface water using hybrid processes — Adsorption on PAC and ultrafiltration", *Desalination*, **162**(04), 23-31.
- Mozia, S., Tomaszewska, M. and Morawski, A.W. (2005), "Studies on the effect of humic acids and phenol on adsorption-ultrafiltration process performance", *Water Res.*, **39**(2-3), 501-509.
- Nieuwenhuijsen, M.J. (2005), "Adverse reproductive health effects of exposure to chlorination disinfection by products", *Global Nest*, **7**(1), 128-144.
- Peng, X., Luan, Z. and Zhang, H. (2006), "Montmorillonite-Cu(II)/Fe(III) oxides magnetic material as adsorbent for removal of humic acid and its thermal regeneration", *Chemosphere*, **63**(2), 300-306.
- Qin, X., Liu, F., Wang, G. and Weng, L. (2012), "Simultaneous analysis of small organic acids and humic acids using high performance size exclusion chromatography", *J. Separat. Sci.*, **35**(24), 3455-3460.
- Saito, T., Koopal, L.K., van Riemsdijk, W.H., Nagasaki, S. and Tanakat, S. (2004), "Adsorption of humic acid on goethite: Isotherms, charge adjustments, and potential profiles", *Langmuir*, **20**(3), 689-700.
- Sharp, E.L., Jarvis, P., Parsons, S.A. and Jefferson, B. (2006), "The impact of zeta potential on the physical properties of ferric - NOM flocs", *Environ. Sci. Technol.*, **40**(12), 3934-3940.
- Sutzkover-Gutman, I., Hasson, D. and Semiat, R. (2010), "Humic substances fouling in ultrafiltration processes", *Desalination*, **261**(3), 218-231.
- Woods, G.C., Simpson, M.J., Pautler, B.G., Lamoureux, S.F., Lafrenière, M.J. and Simpson, A.J. (2011), "Evidence for the enhanced lability of dissolved organic matter following permafrost slope disturbance in the Canadian high arctic", *Geochimica Et Cosmochimica Acta*, **75**(22), 7226-7241.
- Xia, S., Nan, J., Liu, R. and Li, G. (2004), "Study of drinking water treatment by ultrafiltration of surface water and its application to china", *Desalination*, **170**(1), 41-47.
- Xiao, F., Xiao, P., Zhang, W.J. and Wang, D.S. (2013), "Identification of key factors affecting the organic fouling on low-pressure ultrafiltration membranes", *J. Membr. Sci.*, **447**(22), 144-152.
- Ye, M., Zhang, H., Wei, Q., Lei, H., Yang, F. and Zhang, X. (2006), "Study on the suitable thickness of a PAC-precoated dynamic membrane coupled with a bioreactor for municipal wastewater treatment", *Desalination*, **194**(1), 108-120.
- Yoon, K., Kim, K., Wang, X., Fang, D., Hsiao, B.S. and Chu, B. (2006), "High flux ultrafiltration membranes based on electrospun nanofibrous porous scaffolds and chitosan coating", *Polymer*, **47**(7), 2434-2441.
- Zularisam, A.W., Ismail, A.F. and Salim, R. (2006), "Behaviours of natural organic matter in membrane filtration for surface

water treatment — A review”, *Desalination*, **194**(1-3), 211-231.

CC